Modern Physics Letters B
Vol. 33, No. 17 (2019) 1950187 (9 pages)

DOI: 10.1142/S0217984919501872

World Scientific
www.worldscientific.com

Tunable gallium nitride-based devices for ultrafast signal processing

Peng Xie[*,†,‡,‖], Yu Wen[§], Wenqiang Yang[*,‖], Zishen Wan[†,‡,**],
Jiarui Liu[¶], Xinyu Wang[*,‖], Siqi Da[‖] and Yishan Wang[*,‖]

[*]*State Key Laboratory of Transient Optics and Photonics,*
Xi'an Institute of Optics and Precision Mechanics (XIOPM),
Chinese Academy of Sciences (CAS), Xi'an 710119, China
[†]*Department of Mechanical Engineering,*
Massachusetts Institute of Technology, Cambridge 02139, USA
[‡]*School of Engineering and Applied Sciences,*
Harvard University, Cambridge 02138, USA
[§]*National University of Defence Technology, Changsha 410073, China*
[¶]*Sun Yat-Sen University, Guangzhou 510000, China*
[‖]*University of Chinese Academy of Sciences, Beijing 100049, China*
[**]*zishenwan@g.harvard.edu*

Received 8 February 2019
Revised 11 March 2019
Accepted 18 March 2019
Published 17 May 2019

In this paper, we propose a micro-ring resonator model based on gallium nitride (GaN) and graphene, which exhibits tunable properties of nonlinearity. It provides a great bandwidth covering from visible to telecommunication band. Especially, based on the characteristic of GaN, it has unique advantages in shorter wavelength, which is used for demonstrating the ultrafast signal processing including wavelength conversion, temporal amplification and pulse compression. Moreover, the tunable signal processing is achieved via the method of applying additional bias voltage to graphene without changing the geometric dimension of the device. These results have significant potential applications of nonlinear optics and optical communications.

Keywords: Gallium nitride; graphene; waveguides; ultrafast signal processing.

1. Introduction

In the past decade, nanoscale devices open the door of nonlinear and quantum optics, which attract increasing attention. Silicon photonics is considerably popular for the natural extension of integrated electronic circuits.[1–3] Despite silicon photonics exhibits many excellent performances, its utility in broadband applications is limited for its 1.1 eV band gap.[4] A platform with wider bandwidth

[**]Corresponding author.

is extremely meaningful to linear and nonlinear optics research, particularly at shorter wavelengths, such as ultraviolet and visible regions. Therefore, III–V nitrides are regarded as key materials to optics field for the unique property in the visible-ultraviolet wavelength range. Meanwhile, GaN enters into the vision of researchers and is recognized as one of the most important semiconductor materials after silicon.[5–8] It exhibits wide band gap and allows nonlinear optics across a large bandwidth (from visible to telecommunication wavelengths) in a CMOS-compatible platform.[9–11] What is more, it has high power handling capabilities and low propagation loss. Additionally, GaN can be grown on sapphire substrates allowing for low microwave loss compared with silicon-based integrated photonics and the fabrication technology is very mature.[12,13] Especially, for the nonlinear Kerr coefficient of GaN is 7.3×10^{-14} cm^2 W^{-1}, it means a good nonlinearity potential, which make GaN more attractive for nonlinear photonics field. Thus, the GaN is considered to develop device for applications of data transmission and communication.[14,15] On the other hand, graphene is a two-dimensional substance of carbon with high electron migration speed,[16–18] has attracted great attention for its complementary metal-oxide semiconductor compatibility.[19–21] A monolayer of graphene possesses a much stronger inter-band optical transition, which is widely used in optoelectronic devices such as optical modulators,[22,23] photodetectors[24] and transistors.[25,26] Moreover, graphene exhibits large nonlinear refractive index (10^{-7} cm^2 W^{-1}), which makes it as an attractive material candidate for photonic devices. Thus, combining GaN and graphene is a new way to develop novel devices, which will make full use of two materials. For previous devices, the performance is always determined after the structure being fixed. This fact limits the value of devices in practical system, which means that they just could be used for limited purposes. However, the devices with tunable properties are pursued for their practical value in researchers' mind, which can be used for different conditions and meeting various requirements of system. It will contribute to the flexibility and the practicability of system. Actually, graphene provides a chance to tunable devices, for the properties of graphene can be adjusted by additional bias voltage. Thus, graphene-covered devices open the door of tunable device field and break the limitation of conventional devices. In recent years, increasingly researches about graphene–SOI waveguides have been reported,[21,22,27] which present these devices' properties, such as optical field distribution, nonlinear efficient, dispersion and so on, could be optimized by extra bias voltage even when the geometric structure is fixed.[27]

In this work, a novel micro-ring resonator based on GaN and graphene is proposed. The tunability of dispersion and working wavelength range are demonstrated by loading extra bias voltage and a wide bandwidth covering from 380 nm to 1620 nm is realized. Furthermore, we achieve the ultrafast signal processing based on the device including wavelength conversion, temporal amplification and pulse compression, which exhibits significance in data transmission and communication. It will be helpful to build a communication system with a high speed and strongly stability.

2. The Micro-Ring Resonator Model Based on Graphene-GaN

As is well known, nanoscale devices are developed with a high speed for the design flexibility. The mature CMOS technology makes it attractive for many applications, such as photonic integration, detector, modulator, and sensor. In this work, we suppose to create a GaN-based device for ultrafast signal processing. As is mentioned in Introduction, GaN and graphene exhibit unique optical–electrical characteristic. Therefore, we have simulated the GaN-based waveguide with graphene layer for the optical mode by finite element method. The result is presented in Fig. 1. As we can see from the picture, the light power is strongly restricted in the core material.

Here, we propose a micro-ring resonator combining graphene and GaN shown in Fig. 2, which can be used for nonlinear optics research in visible telecommunication region. Figure 2(a) presents the 3D structure of the GaN-based device, a monolayer graphene is covered on GaN ring and a bias voltage is applied to graphene layer. The width and height of core material are set as $w_{\text{core}} = 0.8\ \mu\text{m}$ and $h_{\text{core}} = 0.6\ \mu\text{m}$, respectively. In addition, the radius of the ring and the gap between ring with waveguide are set as $R = 40\ \mu\text{m}$ and $L = 1.5\ \mu\text{m}$. Figure 2(b) presents the second-order dispersion of the device, it keeps minus with the wavelength range from 380 nm to 1620 nm, which means it can reach phase-match in a great bandwidth. Figures 2(c) and 2(d) present the status of off resonance or on resonance, respectively.

The optical conductivity of graphene can be controlled by additional measures, such as extra bias voltage or chemical doping.[28–30] To apply bias voltage to graphene layer is the most straightforward path to adjust it for graphene-related devices, which could be calculated by the Kubo formula.[27,29–31] As is shown in Kubo formula, chemical potential is equivalent to biased voltage, which is applied to value simulation in this work. With the optical conductivity of graphene modified dynamically, the effective index of the graphene-related waveguide will obtain a variation, which will directly contribute to the optimization of parameters, such as nonlinear efficient, light confinement, and dispersion.[27] Especially, tunable second-order dispersion will be obtained without changing the geometrical structure by loading different bias voltages to graphene layer, which is shown in Fig. 3.

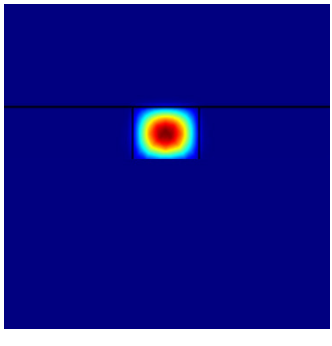

Fig. 1. (Color online) TM mode for the model combining GaN and graphene.

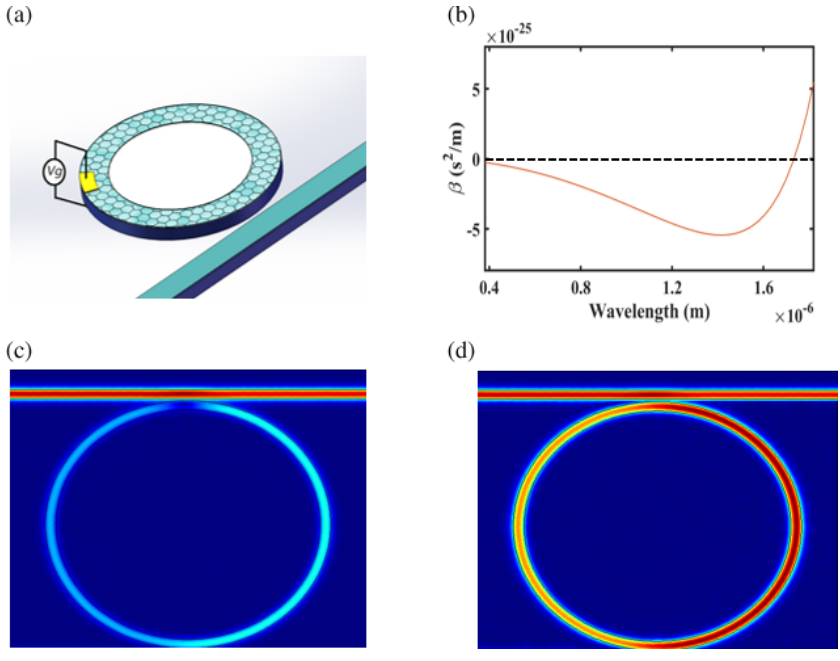

Fig. 2. (Color online) (a) Three-dimensional structure. (b) The second-order dispersion of the device. (c) The status of off resonance. (d) The status of on resonance.

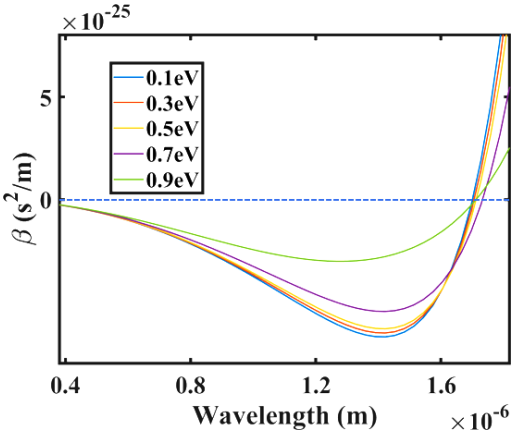

Fig. 3. (Color online) Second-order dispersion of the device under different bias voltages.

In nonlinear optics field, phase-mismatch is an extremely significant spot, which directly relates to the success of the nonlinear parametric processes. Thus, the tunable second-order dispersion plays an important role in nonlinear parametric process, which determines the energy threshold of pump and the phase-match of effective nonlinear effects.[32] According to the results of simulation of Fig. 3, it provides a possibility to create a tunable system for signal processing.

3. Ultrafast Signal Processing Based on the GaN-Based Device

Four-wave mixing (FWM) is an important nonlinear effect and attracts increasing attention, which is widely used for applications in optical parametric amplification and optical parametric oscillator. Here, we focus on ultrafast signal processing based on the degenerate FWM. In this paper, we use this theory to realize wavelength conversion, temporal magnification and pulse compression. The process can be described by the following coupled wave equations:

$$\begin{aligned}
&\frac{\partial A_p}{\partial z} + i\frac{1}{2}\beta_{2p}\frac{\partial^2 A_p}{\partial T^2} - \frac{1}{6}\beta_{3p}\frac{\partial^3 A_P}{\partial T^3} \\
&\quad = -\frac{1}{2}\alpha_p A_p + i\gamma_p |A_p|^2 A_p \\
&\qquad + i2\gamma_p(|A_s|^2 + |A_i|^2)A_p + i2\gamma_p A_s A_i A_p^* \ \exp(i\Delta\beta z), \qquad (1) \\
&\frac{\partial A_s}{\partial z} + i\frac{1}{2}\beta_{2s}\frac{\partial^2 A_s}{\partial T^2} - \frac{1}{6}\beta_{3s}\frac{\partial^3 A_s}{\partial T^3} + d_s\frac{\partial A_s}{\partial T} \\
&\quad = -\frac{1}{2}\alpha_s A_s + i\gamma_s |A_s|^2 A_s \\
&\qquad + i2\gamma_s(|A_p|^2 + |A_i|^2)A_s + i\gamma_s A_p^2 A_i^* \ \exp(-i\Delta\beta z), \qquad (2) \\
&\frac{\partial A_i}{\partial z} + i\frac{1}{2}\beta_{2i}\frac{\partial^2 A_i}{\partial T^2} - \frac{1}{6}\beta_{3i}\frac{\partial^3 A_i}{\partial T^3} + d_i\frac{\partial A_i}{\partial T} \\
&\quad = -\frac{1}{2}\alpha_i A_i + i\gamma_i |A_i|^2 A_i \\
&\qquad + i2\gamma_i(|A_p|^2 + |A_s|^2)A_i + i\gamma_i A_p^2 A_s^* \ \exp(-i\Delta\beta z), \qquad (3)
\end{aligned}$$

where A_j is the amplitude ($j = p, s, i$), Z is the propagation distance, and α_j is the linear loss ($j = p, s, i$). The walk-off parameters for the signal and idler are defined as $d_s = \beta_{1s} - \beta_{1p}$ and $d_i = \beta_{1i} - \beta_{1p}$, respectively. β_n is the nth-order dispersion coefficient, which is calculated via numerical differentiation from $\beta_n = d^n\beta/d\omega^n$.

Figure 4(a) shows the scheme of wavelength conversion based on degenerate FWM in the GaN-based device. A 4 ps pulse of central wavelength at 5.5 μm is considered as input signal and a 2 ps pulse of central wavelength at 1.55 μm is considered as input pump. Signal and pump enter into system and get through polarization controller, respectively. Figures 4(b) and 4(c) presents the temporal waveform of the input signal and input pump, respectively. Figures 4(e) and 4(f) presents frequency spectrum of the input signal and input pump, respectively. Then they are coupled into to GaN-based micro-ring resonator. The idler is selected out by a bandpass filter after FWM effect. Figures 4(d) and 4(g) presents the temporal waveform and frequency spectrum of idler. As we can see from the picture, an output of central wavelength at 1.05 μm is obtained.

As mentioned in section of device design, tunable second-order dispersion will make tunable system of wavelength conversion. Based on the tunable GaN-based

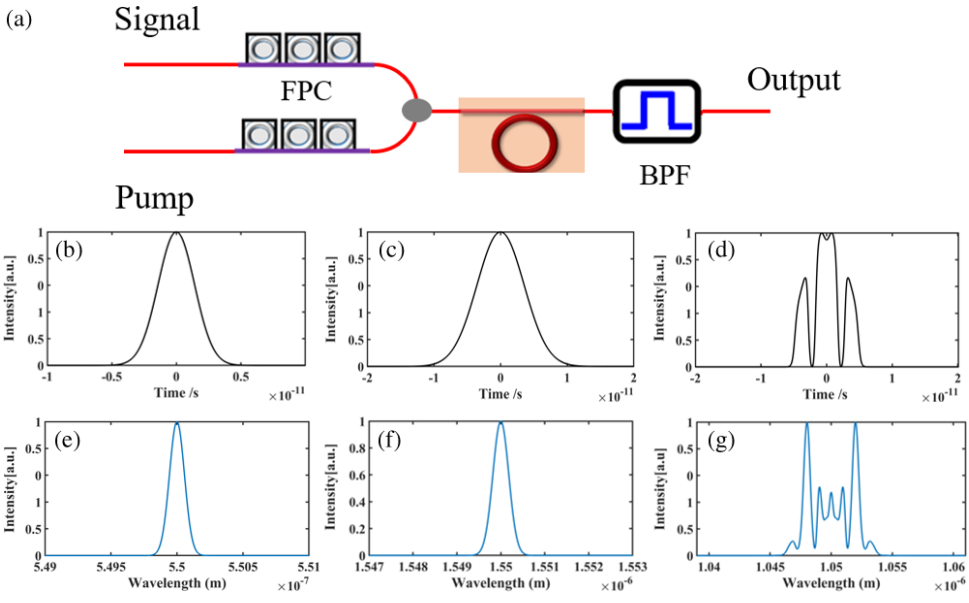

Fig. 4. (Color online) (a) The scheme of wavelength conversion based on FWM in the GaN-based device. (b) Temporal waveform of the input signal. (c) Temporal waveform of the input pump. (d) Temporal waveform of the output signal. (e) Frequency spectrum of input signal. (f) Frequency spectrum of the input pump. (g) Frequency spectrum of the output signal.

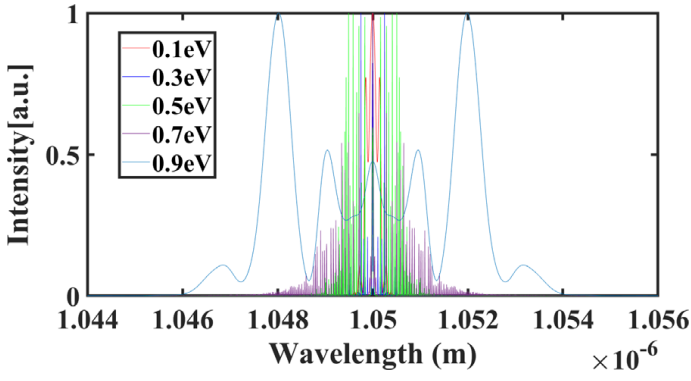

Fig. 5. (Color online) Frequency spectrum of the output under different bias voltages.

micro-ring resonator, the tunable output is achieved, which is shown in Fig. 5. The wavelength range of output is shifted and the different wavelengths exhibit different powers. It means that the tunable second-order dispersion changes the location of phase-match in nonlinear parametric processes. These results have a promising application in signal processing and information transmission.

Figure 6(a) shows the scheme of temporal processing including temporal magnification and pulse compression. After entering into system, signal and pump

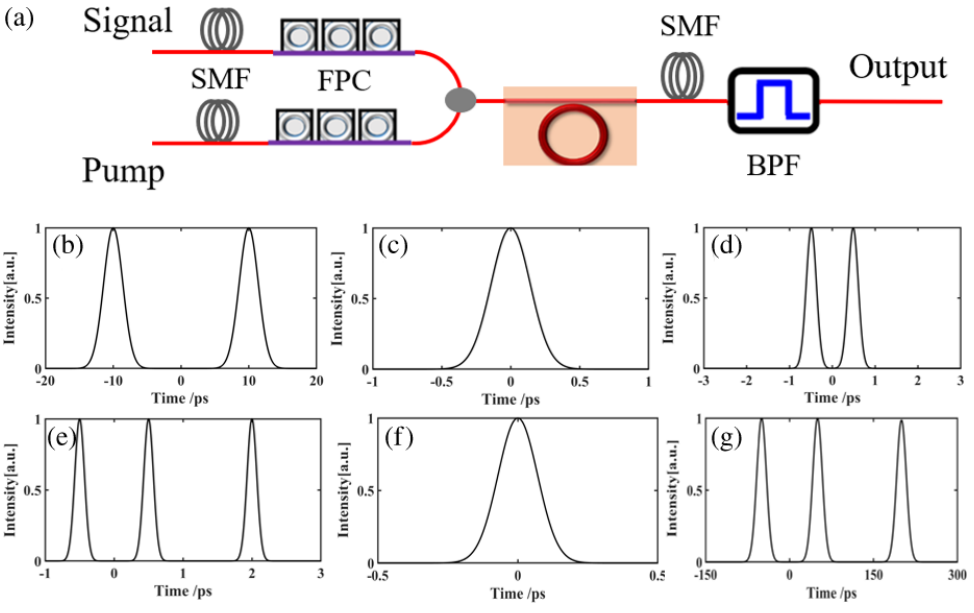

Fig. 6. (Color online) (a) The scheme of temporal processing based on FWM in the GaN-based device. (b) Temporal waveform of the input signal of pulse compression. (c) Temporal waveform of the pump of pulse compression. (d) Temporal waveform of the output signal of pulse compression. (e) Temporal waveform of the input signal of temporal magnification. (f) Temporal waveform of the pump of temporal magnification. (g) Temporal waveform of the output signal of temporal magnification.

get through single mode fiber and polarization controller in order, then they are coupled into the GaN-based micro-ring resonator. The idler also gets through single mode fiber and is selected out by bandpass filter as output. Single mode fiber is used for providing dispersion or dispersion compensation.

Figure 6(b) presents a signal of two 3 ps pulses separated by 20 ps. It gets through a 1 km single mode fiber and polarization controller in order. Figure 6(c) presents a pump of a 500 fs pulse. It also gets through a 2 km single mode fiber and polarization controller in order. Then, the signal and the pump are combined by coupler and enter into the micro-ring resonator. The idler gets through 50 m single mode fiber and is selected by bandpass filter, which is shown in Fig. 6(d). A compression factor of 20× is realized. What is more, Fig. 6(e) presents a signal of three 200 fs pulses. It gets through a 100 m single mode fiber and polarization controller in order. Figure 6(f) presents a pump of a 100 fs pulse. It also gets through a 200 m single mode fiber and polarization controller in order. Then, the signal and the pump are combined by coupler and enter into the micro-ring resonator. The idler gets through 100 km single mode fiber and is selected by bandpass filter, which is shown in Fig. 6(g). A magnification factor of 100× is realized. These results exhibit extremely important research value for signal processing field.

4. Conclusions

In this paper, a novel GaN-related micro-ring resonator covering with graphene is proposed, which is able to work in a great bandwidth from the visible to telecommunication band. Based on the method of loading the extra bias voltage, the tunability of performance of the device is demonstrated. Meanwhile, the tunable wavelength conversion is realized based on the device. Moreover, temporal magnification and pulse compression of ultrafast signal are achieved. These results provide significant reference for further research of signal processing, promoting an attractive potential in data transmission and optical communication.

Acknowledgments

This work was supported by the Strategic Priority Research Program of the Chinese Academy of Sciences (Grant No. XDB24030600) and the China Scholarship Council.

References

1. R. Kirchain and L. Kimerling, *Nat. Photonics* **1** (2007) 303.
2. D. Agostino, G. Carnicella, C. Ciminelli, P. Thijs, P. J. Veldhoven, H. Ambrosius and M. Smit, *Opt. Express* **23** (2015) 25143.
3. W. Bogaerts, P. D. Heyn, T. V. Vaerenbergh, K. D. Vos, S. K. Selvaraja, T. Claes, P. Dumon, P. Bienstman, D. V. Thourhout and R. Baets, *Laser Photonics Rev.* **6** (2012) 47.
4. A. W. Bruch, C. Xiong, B. Leung, M. Poot, J. Han and H. X. Tanga, *Appl. Phys. Lett.* **107** (2015) 141113.
5. T. Kuykendall, P. J. Pauzauskie, Y. F. Zhang, J. Goldberger, D. Sirbuly, J. Denlinger and P. Yang, *Nature* **3** (2004) 526.
6. Z. Y. Al Balushi, K. Wang, R. K. Ghosh, R. A. Vilá, S. M. Eichfeld, J. D. Caldwell, X. Y. Qin, Y. C. Lin and J. A. Robinson, *Nat. Mater.* **15** (2016) 1166.
7. S. Zhao, A. T. Connie, M. H. T. Dastjerdi, X. H. Kong, Q. Wang, M. Djavid, S. Sadaf, X. D. Liu, I. Shih, H. Guo and Z. Mi, *Sci. Rep.* **5** (2015) 8332.
8. X. F. Wu, J. Lee, V. Varshney, J. L. Wohlwend, A. K. Roy and T. F. Luo, *Sci. Rep.* **6** (2016) 22504.
9. S. R. Bowman, C. G. Brown and B. Taczak, *Opt. Mater. Express* **8** (2018) 1093.
10. R. X. Yan, D. Gargas and P. D. Yang, *Nat. Photonics* **3** (2009) 569.
11. T. N. Oder, K. H. Kim, J. Y. Lin and H. X. Jiang, *Appl. Phys. Lett.* **84** (2004) 466.
12. Y. F. Zhang, L. M. Knight, E. Engin, I. M. Watson, M. J. Cryan, E. Gu, M. G. Thompson, S. Calvez, J. L. Brien and M. D. Dawson, *Appl. Phys. Lett.* **99** (2011) 161119.
13. M. Tchernycheva, A. Messanvi, A. L. Bugallo, G. Jacopin, P. Lavenus, L. Rigutti, H. Zhang, Y. Halioua, F. H. Julien, J. Eymery and C. Durand, *Nano Lett.* **14** (2014) 3515.
14. A. David, C. Meier, R. Sharm, F. S. Dian, S. P. DenBaars, E. Hu, S. Nakamur and C. Weisbuch, *Appl. Phys. Lett.* **87** (2005) 101107.
15. R. Hui, S. Taherion and Y. Wan, *Appl. Phys. Lett.* **82** (2003) 1326.
16. X. Gan, R. Shiue, Y. Gao, I. Meric, T. F. Heinz, K. Shepard, J. Hone, S. Assefa and D. Englund, *Nat. Photonics* **7** (2013) 883.
17. J. Wang, Z. Cheng and X. Li, *Adv. Cond. Matter Phys.* **10** (2018) 1.

18. M. Liu, X. Yin and X. Zhang, *Nano Lett.* **12** (2012) 1482.
19. K. S. Kim, Y. Zhao, H. Jang, S. Y. Lee, J. M. Kim, K. S. Kim, J. Ahn, P. Kim, J. Choi and B. H. Hong, *Nature* **457** (2009) 706.
20. A. Reina, X. Jia, D. Nezich, H. Son, V. Bulovic, M. S. Dresselhaus and J. Kong, *Nano Lett.* **9** (2009) 30.
21. Y. Meng, S. W. Ye, Y. J. Shen, Y. M. Yang and M. L. Gong, *IEEE Photonics J.* **10** (2018) 6600217.
22. Y. Meng, F. Hu, Y. J. Shen, Y. M. Yang and M. L. Gong, *Sci. Rep.* **8** (2018) 13362.
23. V. Sorianello and M. Midrio, *Opt. Express* **23** (2015) 6478.
24. Y. Gao, L. Tao, H. K. Tsang and C. Shu, *Appl. Phys. Lett.* **112** (2018) 211107.
25. T. Georgiou, R. Jalil, B. D. Belle, L. Britnell, R. V. Gorbachev, S. V. Morozov, Y. Kim, A. Gholinia, S. J. Haigh, O. Makarovsky, L. Eaves, L. A. Ponomarenko, A. K. Geim, K. S. Novoselov and A. Mishchenko, *Nat. Nanotechnol.* **8**(2) (2013) 100.
26. D. Jena, *Proc. IEEE* **101** (2013) 1585.
27. P. Xie, M. T. Xue, Y. Wen, X. F. Li, X. Y. Wang, H. Y. Yin, C. Z. Du, J. R. Liu and J. H. Liu, *M. Phys. Lett. B* **10** (2019) 1950053.
28. A. A. Balandin, S. Ghosh, W. Bao, I. Calizo, D. Teweldebrhan, F. Miao and C. N. Lau, *Nano Lett.* **8** (2008) 902.
29. G. W. Hanson, *J. Appl. Phys.* **103** (2008) 064302.
30. P. Xie *et al.*, *Jpn. J. Appl. Phys.* (2019), https://doi.org/10.7567/1347-4065/ab0c52.
31. Z. Song, H. Liu, N. Huang and Z. Wang, *J. Appl. Phys.* **51** (2018) 095108.
32. P. Xie, Q. Sun, L. Wang, Y. Wen, X. Wang, G. Wang, C. Zeng, M. Liu, Z. Ge and Z. Lu, *Appl. Phys. Express* **11** (2018) 082204.